15. H. Keppler, C. A. McCammon, D. C. Rubie, *Am. Mineral.* **79**, 1215 (1994).
16. A. Wall, G. D. Price, S. C. Parker, *Mineral. Mag.* **50**, 693 (1986).
17. Y. Kudoh, C. T. Prewitt, L. W. Finger, *Geophys. Res. Lett.* **17**, 1481 (1990).
18. K. Ullrich, K. Langer, K. D. Becker, *Phys. Chem. Miner.* **29**, 409 (2002).
19. H. Keppler, N. Bagdassarov, *Chem. Geol.* **158**, 105 (1999).
20. M. N. Taran, K. Langer, *Neues Jahrb. Mineral. Abh.* **172**, 325 (1998).
21. A. P. van den Berg, D. A. Yuen, V. Steinbach, *Geophys. Res. Lett.* **28**, 875 (2001).
22. C. Matyska, J. Moser, D. A. Yuen, *Earth Planet. Sci. Lett.* **125**, 255 (1994).
23. C. Matyska, D. A. Yuen, *Earth Planet. Sci. Lett.* **234**, 71 (2005).
24. Y. Xu *et al.*, *Phys. Earth Planet. Inter.* **143-144**, 321 (2004).
25. S. Lundin *et al.*, *Phys. Earth Planet. Inter.* **168**, 97 (2008).
26. F. Deschamps, J. Trampert, *Earth Planet. Sci. Lett.* **222**, 161 (2004).
27. This work was supported by German Science Foundation (DFG; Leibniz award to H.K.). A. Audétat took the photographs of the samples at high pressure.

Supporting Online Material
www.sciencemag.org/cgi/content/full/322/5907/1529/DC1
Materials and Methods
References and Notes

13 August 2008; accepted 23 October 2008
10.1126/science.1164609

Quasi-Periodic Bedding in the Sedimentary Rock Record of Mars

Kevin W. Lewis,[1]* Oded Aharonson,[1] John P. Grotzinger,[1] Randolph L. Kirk,[2] Alfred S. McEwen,[3] Terry-Ann Suer[1]

Widespread sedimentary rocks on Mars preserve evidence of surface conditions different from the modern cold and dry environment, although it is unknown how long conditions favorable to deposition persisted. We used 1-meter stereo topographic maps to demonstrate the presence of rhythmic bedding at several outcrops in the Arabia Terra region. Repeating beds are ~10 meters thick, and one site contains hundreds of meters of strata bundled into larger units at a ~10:1 thickness ratio. This repetition likely points to cyclicity in environmental conditions, possibly as a result of astronomical forcing. If deposition were forced by orbital variation, the rocks may have been deposited over tens of millions of years.

Sedimentary rocks record surface and environmental conditions throughout the history of Mars (*1*, *2*). Landed missions have studied a few locations in detail, but most deposits remain accessible only from orbital data. The High Resolution Imaging Science Experiment (HiRISE) (*3*) has revealed meter-scale bedding in the rocks at many locations. Stereo observations allow the three-dimensional structure of these stratified outcrops to be determined, from which bedding orientations and true thicknesses can be calculated. Here, we report on the measurement of several stratified deposits in the Arabia Terra region that contain highly rhythmic bedding and may record a history of orbitally forced variations in surface conditions. Previous attempts have been made to correlate layers within the north polar ice cap of Mars to the most recent orbital history (*4*, *5*). In contrast, the rocks of Arabia Terra record ancient surface conditions.

The intracrater layered deposits of Arabia Terra are thick sequences of sedimentary rocks distributed widely across Mars from 350°E to 30°E and from the equator up to 25°N (*6*). Although the deposits are separated by large distances, the region in which they occur is greater than 500 km by 1000 km in area. Most sequences are several hundred meters thick and have eroded back to remnant mounds on the floors of large craters, natural locations for both deposition and preservation. Many deposits have a stair-stepped morphology, with the differential resistance of the outcrops highlighting their stratified internal structure (*1*). The origin of these sedimentary rocks is uncertain, although there is a general lack of valley incision in western Arabia Terra (*7*, *8*), and there is no observed evidence for fluvial channels within these deposits. Although erosion may have removed overlying strata (*8*), the craters we studied do not have breached or heavily incised rims and show little evidence for lacustrine processes.

Among the craters containing light-toned layered deposits in Arabia Terra, four have adequate stereo coverage to make quantitative measurements of the stratigraphy. These sedimentary sequences contain tens to hundreds of beds of similar morphology with planar and parallel bedding. Faults offset the stratigraphy in places, but we have avoided these areas in our analysis. Extensive aeolian erosion has revealed the thick sections and also provides a clue to the depositional origin of the rocks. Few craters are observed on the light-toned deposits, and little talus is observed at the base of steep slopes, which suggests that the deposits are weakly lithified and consist of grains fine enough to be transported away by modern aeolian activity. The striking differential resistance to erosion seen across each bed points to a repeated change in the depositional environment as the strata were formed.

To assess the structure of layered deposits, we created digital terrain models (DTMs) with 1-m grid spacing from HiRISE stereo images, using the techniques of (*9*). These products were controlled to the Mars Orbiter Laser Altimeter (MOLA) data set as part of the generation process; they have a vertical accuracy of <1 m, allowing analysis of meter-scale bedding (table S1). Figure 1 shows a cross section along one outcrop, demonstrating that 10-m-scale layers are well resolved in the stereo DTM. Although the apparent thicknesses are variable in plan view, the true bed thicknesses are highly regular when the erosional topography and southward dip are accounted for. Accordingly, bedding orientations were calculated via linear regression and were typically derived from hundreds of individual topographic data points, resulting in a precision of <0.5° on the dip of a bed. We made measurements throughout each section to ensure that the orientation was consistent. At the Becquerel crater site, a slight change in bedding orientation was observed and accounted for within the upper 80 m of section. We then identified bed boundaries in plan view and projected each to a common reference frame using the measured orientation of the outcrop.

For each of the Arabia sites, the bed thicknesses are tightly clustered around a mean value (Table 1 and tables S2 to S6). The thinnest beds are still above the resolution limits of both the images and the DTMs, which have a pixel scale of 1 m but typically sample the stratigraphic col-

Table 1. Bed thicknesses measured from HiRISE stereo topographic data at four outcrops in the Arabia Terra region of Mars. Each location shows regularly cyclic sequences, possibly indicative of depositional control by an external climate cycle. The characteristic thicknesses vary between sites, which suggests that the deposits formed in isolation rather than as a widespread regional geologic unit.

Crater	Location	Number of beds measured	Mean thickness ± SD (m)
Becquerel (beds)	22°N, 352°E	66	3.6 ± 1.0
Becquerel (bundles)	22°N, 352°E	10	35.5 ± 9.2
Crommelin	5°N, 350°E	8	19.6 ± 4.0
Unnamed	8°N, 353°E	14	9.7 ± 1.5
Unnamed	9°N, 359°E	10	12.6 ± 2.6

[1]Divison of Geological and Planetary Sciences, California Institute of Technology, 150-21, Pasadena, CA 91125, USA. [2]U.S. Geological Survey, 2255 N. Gemini Drive, Flagstaff, AZ 86004, USA. [3]Lunar and Planetary Laboratory, University of Arizona, Tucson, AZ 85721, USA.

*To whom correspondence should be addressed. E-mail: klewis@gps.caltech.edu

umn at even finer intervals (~0.1 m) because of the slope of the outcrops. Although the scale of the bedding varies from site to site, it is consistent among outcrops at the same location. Within the two unnamed craters at 8°N, 353°E and 9°N, 359°E, the characteristic thicknesses are about 10 and 13 m, respectively. At Crommelin crater (5°N, 350°E), beds are 20 m thick, whereas Becquerel (22°N, 352°E) shows two scales of stratification at 3.6 and 36 m. The distribution of bed thicknesses at each location is consistent with a normal distribution via the Kolmogorov-Smirnov test. Alternative hypotheses that the data are distributed either exponentially or according to a power law can be rejected (*10*). We consider possible interpretations of these observed distributions below.

We used spectral analysis of the stratigraphic records to further assess the periodicity of the bedding at these locations. Image grayscale values and DTM slope profiles both provide a continuous record of the stratigraphy. In three of the four locations, we analyzed the image brightness record, whereas at the 9°N, 359°E site, slope values provided a better record because of unfavorable lighting conditions. The data were sampled from the orthorectified images or DTM and were then corrected for the structural dip and topography. To obtain a uniformly spaced record, we resampled the record in the stratigraphic reference frame to the mean spacing of the data (~0.1 m in all four cases). We derived spectral estimates via the multitaper method of (*11*), which were then assessed relative to a first-order autoregressive (red noise) background. We used the robust estimation technique of (*11*) to model the red noise component of the data and derive corresponding confidence levels. Spectral peaks exceeding these thresholds indicate that a quasi-

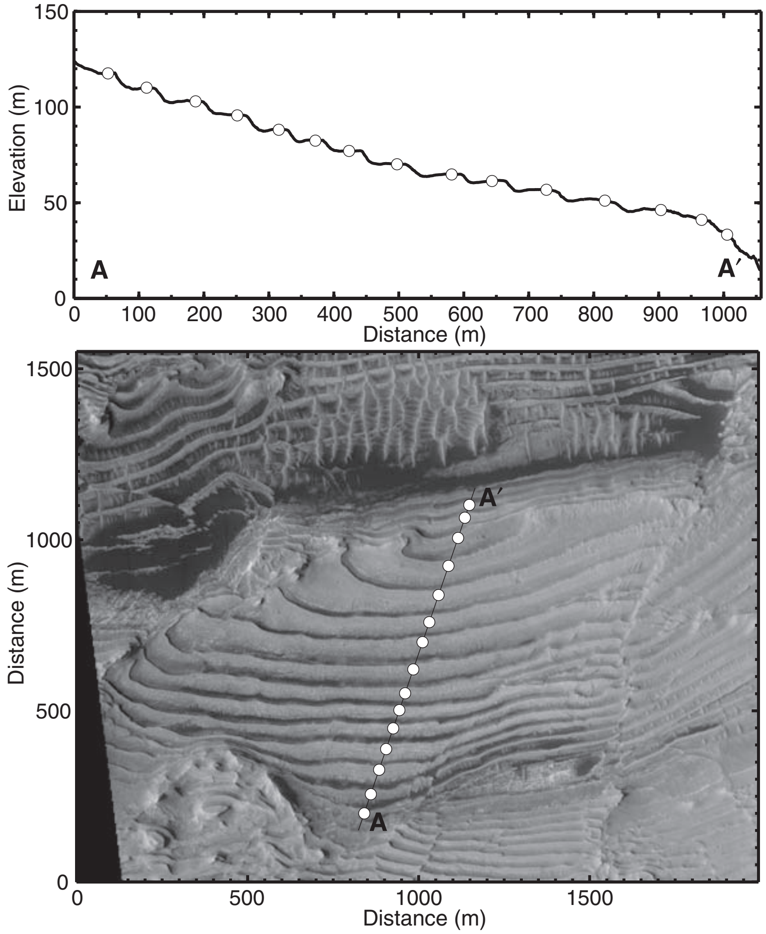

Fig. 1. Topographic profile across one rhythmically bedded outcrop, showing that strata are well resolved in the stereo DTM. Although the beds have varying apparent thicknesses in the original images, the true thicknesses are quasi-periodic when the erosional topography and southward dip is properly accounted for. The lower panel is an orthogonal projection of HiRISE image PSP_002733_1880 and shows the location of profile A-A′ along with the corresponding bed positions.

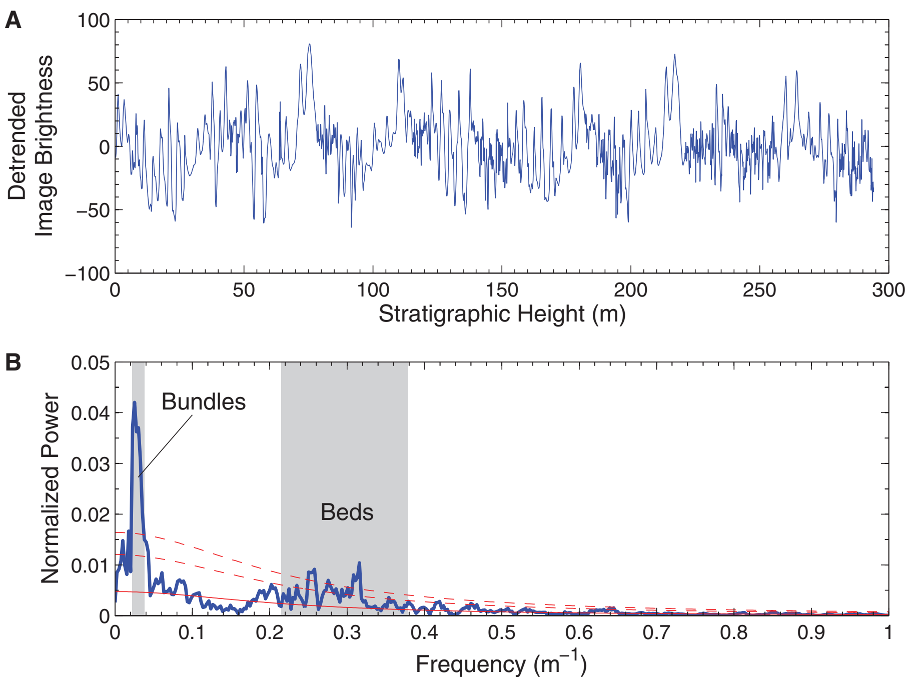

Fig. 2. (**A**) Detrended image grayscale levels of the Becquerel crater outcrop, topographically corrected and resampled at a uniform interval of 0.1 m in the stratigraphic column. (**B**) Power spectrum of the Becquerel crater stratigraphy. Estimated red noise background (red solid line) and 95% and 99% confidence levels (red dashed lines) are indicated. Shaded regions indicate the 1σ range of bed and bundle thickness measurements, which correspond well to the two regions where power exceeds the 99% confidence level, indicating quasi-periodicity at both scales.

periodic component is nonrandom with the specified confidence. The spectra showed peaks that exceeded the 99% confidence levels at the measured bedding scales for all sites except Crommelin crater, where the excess power only surpassed the 95% threshold. In the Becquerel spectrum, power exceeded the 99% confidence level relative to the estimated background at both 3 to 4 m and 30 to 40 m, demonstrating statistically significant quasi-periodicity in the Becquerel stratigraphy at both scales (Fig. 2).

The observation of rhythmic layering on Mars at multiple locations across the Arabia region constitutes evidence of cyclic variation in ancient surface conditions. The different scales measured, along with the varying morphologies observed between sites and the dearth of similar deposits on the intervening plains in Arabia (*12*), suggest that these deposits formed in isolation rather than as part of a regionally extensive sedimentary unit. Still, the presence of several regularly cyclic sequences within this region of Mars hints at a common external driver, with the local conditions of each sedimentary basin influencing the expression of climate cycles in the stratigraphy.

From orbit, it is difficult to determine the nature of the prominent bed boundaries that give rise to the alternating pattern of erosional resistance. Each erosional step may record discrete or continuous changes in the bulk composition or lithification history of the sediments, overlain on a steady background sedimentation rate. Alternatively, the deposition rate may have varied over each cycle, with episodes of relatively low accumulation leading to more complete induration of the sediment. In either case, quasi-periodic bedding will result when the sediment accumulation rate is roughly constant when averaged over each cycle. With either model, the observed periodicity in stratigraphic position represents a record of cyclicity in time.

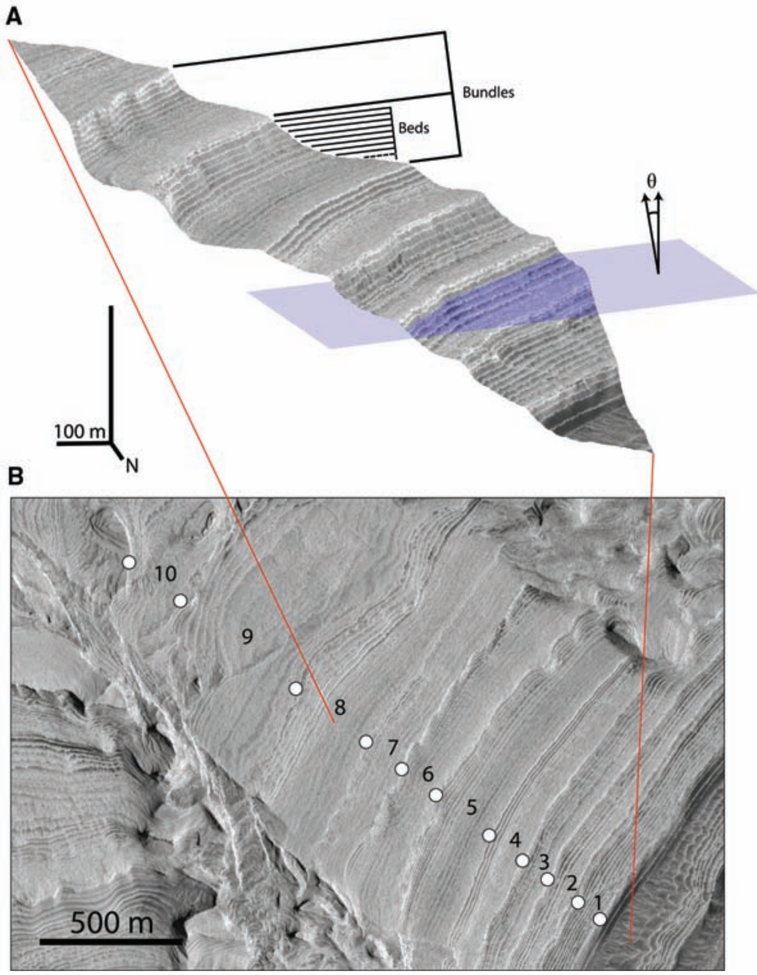

Fig. 3. (**A**) Three-dimensional view of the stratified deposit within Becquerel crater. This location shows two scales of quasi-periodic bedding, marked as beds and bundles. The ratio of these characteristic thicknesses is a potential clue to the forcing mechanisms responsible for the cyclicity seen in the rocks. The blue plane indicates the best-fit orientation of the bedding, which has a dip of ~3°. To obtain true thicknesses, it is necessary to account for both the erosional morphology and the tilt of the bedding from horizontal (indicated by θ). HiRISE image PSP_001546_2015 is shown draped over digital stereo topography. Scale bars, 100 m (both horizontal and vertical). (**B**) Plan view of HiRISE image PSP_001546_2015, showing context for (A); north is down. Numbers mark the boundaries between successive bundles as revealed in the topography.

An alternative depositional model is that each bed was laid down by discrete, aperiodic events of similar magnitude. This is seen, for example, on Earth in the flood deposits of glacial Lake Missoula, where outbursts of comparable magnitude created repeating beds of similar thickness (*13*). Two observations argue against this possibility in Arabia Terra. First, the bundling of strata into repeating packages seen in Becquerel crater would require an unlikely additional level of incidental cyclicity. Second, the apparent lack of coarse sediment, channel incision, or erosional unconformities argues against fluvial emplacement of these several-meter-thick beds. Emplacement of a bed in this scenario must occur in a single depositional event to be time scale–independent. This requirement likely rules out formation by individual dust storms, for instance, as current dust deposition rates are on the order of only micrometers per year (*14*). It is impossible to rule out any scenario without knowing the precise relationship between time and depth. However, we find this case improbable given the bundling seen at Becquerel crater, the volumes of sediment required, and the lack of evidence for aqueous deposition.

The nature of the sedimentation process that deposited the Arabia layers remains uncertain. However, the observation of regularly cyclic bedding rules out processes that occur in a purely stochastic manner, including volcanism and impact cratering. Such events recorded at random intervals within a stratigraphic column are expected to result in an exponential distribution of intervals (*15*). Further, the size-frequency distributions of many stochastic depositional processes are skewed toward smaller events and can be described in many cases by a power law. Such processes include turbidites, flood events, landslides, volcanic eruptions, and impacts [(*16*, *17*) and references therein]. As both power-law and exponential distributions can be statistically rejected for several of the Arabia sites, a stochastic process of this nature is unlikely without forcing by environmental cyclicity.

On Earth, periodic stratification in the rock record is often associated with cyclic driving mechanisms, which influence the deposition and preservation of sediments. Tidal, seasonal, solar, and orbital cycles have all been documented in sedimentary records (*18*–*20*). Quasi-periodic climate cycles on Earth can also arise from internal atmospheric, ocean, and ice sheet dynamics, without an obvious external forcing function (*20*). On Mars, the likelihood of such internally generated cycles is diminished in the absence of oceans, wet-based ice sheets, and biological feedbacks (*21*). Martian global dust storms may be quasi-periodic, although at shorter, interannual time scales (*22*).

In analogy to Earth, the strongest periodic signals on Mars arise at diurnal, annual, and orbital frequencies, all of which cause large variations in local surface conditions. As on Earth, these cyclic forcing mechanisms are dominant at periods shorter than ~10 years and longer than a few tens of thousands of years (*19*). The thickness of the beds in Arabia argues against deposition on diurnal or annual time scales. Annual accumulation of more than 10 m of sediment would represent an extremely high deposition rate and would imply that the kilometer-thick deposits accumulated in as little as tens of years. In contrast, deposition at orbital frequencies (~100,000 years) assumes a modest average accumulation rate of ~100 μm per year. This value allows for alternating accumulation and erosion of sediment on shorter time scales, requiring only that the net deposition is roughly constant over long time scales.

Bundling within rhythmic sequences has been a useful indicator of Milankovitch forcing on Earth. In particular, the 5:1 frequency ratio of the precession cycle to the eccentricity cycle for Earth has been observed in the rock record (*19*, *23*). A hierarchy of this type can be used not only to confirm the influence of a periodic forcing mechanism, but also to translate stratigraphic cycles to relative time scales (*24*). At Becquerel crater (Fig. 3), we observed a roughly 10:1 ratio of frequencies over several hundred meters of section, for a total of at least 10 bundles. Individual beds here have a mean thickness of 3.6 ± 1 m, and the bundles are 36 ± 9 m thick. Strata are less distinct near the bottom of each bundle, making it difficult to obtain a precise count for each cycle.

The obliquity of Mars has the largest effect on the global climate, and is one of the most frequently invoked mechanisms for climate change (*2*, *21*, *25*, *26*). The tilt of the planet's spin axis ranges over tens of degrees and can have a strong effect on climate, changing the mean annual insolation even at low latitudes by 10% or more, and affecting the global distribution of volatiles. Among the leading effects, polar condensation of carbon dioxide is expected to reduce atmospheric pressure at low obliquity (*27*). For an aeolian depositional scenario, reduced pressure limits the capacity of the atmosphere to transport sediment (*28*). The obliquity of Mars oscillates with a period of ~120,000 years and is modulated on a time scale of ~1.2 and ~2.4 million years (*29*, *30*). Orbital calculations show that this modulation is expressed more strongly at 2.4 million years for the recent history of Mars, although the ancient history is unknown because of the chaotic nature of the obliquity over long time scales (*31*). As the absolute frequencies of these orbital cycles will not vary greatly over geologic time scales (*30*), this 10:1 ratio in the obliquity cycle is a potential candidate for orbital forcing of the cyclic stratigraphy measured at Becquerel crater. This would imply a formation of one bed per 120,000-year obliquity cycle, one bundle per 1.2-million-year modulation cycle, and deposition of the entire measured section over roughly 12 million years.

The identification of quasi-periodic signals within these layered terrains provides a possible relative chronometer within the martian rock record. Orbital variations stand out as a possible driver of the observed quasi-periodicity, although definitive identification of the cycles involved will require additional information. Likewise, whereas an aeolian scenario provides a clear link to orbital forcing, the specific formation model remains uncertain. Determination of formation time scales ultimately provides a calibration for interpreting the geological history of Mars. With the tentative but reasonable assumption that some water was required to lithify the Arabia deposits, the suggestion of orbital cyclicity implies that a hydrologic cycle may have been active at least intermittently over millions of years. In contrast to the catastrophic surface conditions inferred from impact craters and outflow channels, this strong cyclicity observed in the martian rock record depicts a fundamentally more predictable and regular environment in the ancient past.

References and Notes

1. M. C. Malin, K. S. Edgett, *Science* **290**, 1927 (2000).
2. P. R. Christensen, H. J. Moore, in *Mars*, H. H. Kieffer, B. M. Jakosky, C. W. Snyder, M. S. Matthews, Eds. (Univ. of Arizona Press, Tucson, AZ, 1992), pp. 686–729.
3. A. S. McEwen *et al.*, *J. Geophys. Res.* **112**, E05S02 (2007).
4. J. Laskar, B. Levrard, J. F. Mustard, *Nature* **419**, 375 (2002).
5. S. M. Milkovich, J. W. Head, *J. Geophys. Res.* **110**, E01005 (2005).
6. K. Edgett, *J. Geophys. Res.* **107**, 5038 (2002).
7. M. H. Carr, F. C. Chuang, *J. Geophys. Res.* **102**, 9145 (1997).
8. B. M. Hynek, R. J. Phillips, *Geology* **31**, 757 (2003).
9. R. L. Kirk *et al.*, *J. Geophys. Res.* **113**, E00A24 (2008).
10. By comparing the data to ideal distributions via the Kolmogorov-Smirnov test, the hypothesis that the bed thicknesses were drawn from an exponential distribution can be rejected for four out of five data sets at a 95% confidence level. For a power-law distribution, the null hypothesis can be similarly rejected for all of the data sets. In contrast, a normal distribution is consistent with all of the data sets using this test.
11. M. E. Mann, J. M. Lees, *Clim. Change* **33**, 409 (1996).
12. K. S. Edgett, M. C. Malin, *Geophys. Res. Lett.* **29**, 2179 (2002).
13. J. Waitt, R. B. *J. Geol.* **88**, 653 (1980).
14. G. A. Landis, P. P. Jenkins, *J. Geophys. Res.* **105**, 1855 (2000).
15. B. H. Wilkinson, N. W. Diedrich, C. N. Drummond, E. D. Rothman, *Bull. Geol. Soc. Am.* **110**, 1075 (1998).
16. J. Carlson, J. Grotzinger, *Sedimentology* **48**, 1331 (2001).
17. B. D. Malamud, D. L. Turcotte, *J. Hydrol.* **322**, 168 (2006).
18. A. G. Fischer, *Annu. Rev. Earth Planet. Sci.* **14**, 351 (1986).
19. M. R. House, in *Orbital Forcing Timescales and Cyclostratigraphy*, M. R. House, A. S. Gale, Eds. (Geological Society of London, London, 1995), pp. 1–18.
20. G. Weedon, *Time-Series Analysis and Cyclostratigraphy: Examining Stratigraphic Records of Environmental Cycles* (Cambridge Univ. Press, Cambridge, 2003).
21. H. H. Kieffer, A. P. Zent, in *Mars*, H. H. Kieffer, B. M. Jakosky, C. W. Snyder, M. S. Matthews, Eds. (Univ. of Arizona Press, Tucson, AZ, 1992), pp. 1180–1218.
22. R. Kahn, T. Martin, R. Zurek, S. Lee, in *Mars*, H. H. Kieffer, B. M. Jakosky, C. W. Snyder, M. S. Matthews, Eds. (Univ. of Arizona Press, Tucson, AZ, 1992), p. 1017–1053.
23. W. Schwarzacher, *Earth Sci. Rev.* **50**, 51 (2000).
24. L. A. Hinnov, *Annu. Rev. Earth Planet. Sci.* **28**, 419 (2000).
25. W. R. Ward, B. C. Murray, M. C. Malin, *J. Geophys. Res.* **79**, 3387 (1974).
26. J. W. Head, J. F. Mustard, M. A. Kreslavsky, R. E. Milliken, D. R. Marchant, *Nature* **426**, 797 (2003).
27. F. P. Fanale, J. R. Salvail, *Icarus* **111**, 305 (1994).
28. J. A. Cutts, B. H. Lewis, *Icarus* **50**, 216 (1982).
29. W. R. Ward, in *Mars*, H. H. Kieffer, B. M. Jakosky, C. W. Snyder, M. S. Matthews, Eds. (Univ. of Arizona Press, Tucson, AZ, 1992), pp. 298–320.
30. J. Laskar *et al.*, *Icarus* **170**, 343 (2004).
31. J. Touma, J. Wisdom, *Science* **259**, 1294 (1993).

32. Supported by NASA's Mars Data Analysis Program and by the NASA Earth and Space Science Fellowship program. We thank two anonymous reviewers for helpful comments and suggestions.

Supporting Online Material
www.sciencemag.org/cgi/content/full/322/5907/PAGE/DC1
Tables S1 to S6

16 June 2008; accepted 10 November 2008
10.1126/science.1161870

Photoexcited CRY2 Interacts with CIB1 to Regulate Transcription and Floral Initiation in *Arabidopsis*

Hongtao Liu, Xuhong Yu, Kunwu Li, John Klejnot, Hongyun Yang, Dominique Lisiero, Chentao Lin*

Cryptochromes (CRY) are photolyase-like blue-light receptors that mediate light responses in plants and animals. How plant cryptochromes act in response to blue light is not well understood. We report here the identification and characterization of the *Arabidopsis* CIB1 (cryptochrome-interacting basic-helix-loop-helix) protein. CIB1 interacts with CRY2 (cryptochrome 2) in a blue light–specific manner in yeast and *Arabidopsis* cells, and it acts together with additional CIB1-related proteins to promote CRY2-dependent floral initiation. CIB1 binds to G box (CACGTG) in vitro with a higher affinity than its interaction with other E-box elements (CANNTG). However, CIB1 stimulates *FT* messenger RNA expression, and it interacts with chromatin DNA of the *FT* gene that possesses various E-box elements except G box. We propose that the blue light–dependent interaction of cryptochrome(s) with CIB1 and CIB1-related proteins represents an early photoreceptor signaling mechanism in plants.

Arabidopsis cryptochromes (CRY) mediate light regulation of cell elongation and photoperiodic flowering (*1*, *2*), but the photoactivation mechanism of cryptochrome remains unclear. It has been hypothesized that, similar to other photoreceptors, photoexcited cryptochromes may interact with target proteins to regulate gene expression and physiological